and will give a τ_u of 11 for a ϕ of 40 over a temperature range of -65 to $+165$°F. Figure 3 also shows that there is probably not much purpose in searching for a π_p reduction of less than $0.0005°F^{-1}$, since it represents an equivalent n increase of only 0.034 and 0.031 for pressure ratios of 30 and 40 respectively. This conclusion provides an opportunity to economize by reducing the number of strands that should be tested for data points to evaluate formulation approaches.

Conclusions

For propellant research and development directed towards an application requiring wide-temperature-range throttling, formulation approaches to reducing π_p need be evaluated principally for their effect between ambient and low temperature at high pressure and between ambient and high temperatures at low pressure. Thus, cost savings may be realized because π_p need not be determined over the entire temperature range at all pressures. Because n_T is the controlling parameter for propellant throttlability it is advantageous economically to determine n_T directly instead of indirectly by determining n and π_p values.

Temperature Distribution in Shadowed Lunar Craters

A. S. ADORJAN*
General Electric Company, Houston, Texas

Nomenclature

A = surface area of crater, ft²
A_0 = total surface area of sphere, ft²
A_D = surface area of circle by the intersection of the sphere and the lunar surface, ft²
a = D/h, aspect ratio of crater, diameter/depth
F_{ij} = form factor relating A_i and A_j
J = radiosity at an arbitrary location, Btu/hr-ft²
K_{ij} = kernel of Fredholm's integral equation or normalized form factor in the heat balance equations
$\mathbf{n}$ = crater surface unit normal vector
q = local incident heat flux, Btu/hr-ft²
R = radius of sphere, ft
$\mathbf{S}$ = solar constant, 442 Btu/hr-ft²
$\mathbf{s}$ = solar ray directional unit vector
T = radiation equilibrium temperature, °R
α, ϵ = absorptivity and emissivity of lunar soil
γ = thermal inertia of lunar soil, 750 cm²-sec$^{\frac{1}{2}}$-°C/cal
δ = solar elevation angle
λ = parameter of the integral equation
σ = Stefan-Boltzmann constant, 0.1714×10^{-8} Btu/hr-ft²-°R⁴

Subscripts

1, 2 = sunlit and snadowed regions of crater
s = source

Introduction

AN interest in temperature distribution of lunar topographical features has existed for many years. However, most of the experimental (e.g., Ref. 1) and analytical (e.g., Ref. 2) efforts, limited by the resolution of Earth-based instrumentation, have been concentrated on average temperatures of relatively large surface areas. More detailed experimental data have been obtained by the Surveyor flights, especially by Surveyor III and V.[3,4] Lunar surface temperatures were obtained, however, by indirect methods (through compartment temperature data) limiting the accuracy of results. Furthermore, the crater in which Surveyor III landed was too shallow to exhibit marked "cavity" effect. Significant results have been obtained, however, on the thermal inertia of the lunar soil, indicating a numerical value of 500 cm²-sec $\frac{1}{2}$-°C/cal instead of 750 used previously based on terrestrial measurements.

The present study considers temperature distribution in lunar craters. The governing equations of the heat balance are defined in a set of integral equations. Independent of the depth of the crater, the incident solar radiation is identical for all craters with the same surface area at their openings. By energy consideration, the emitted radiation must also be the same. Consequently, heat emission from deep craters may occur at higher surface temperatures in order to compensate for the decrease in the form factor from the cavity toward the deep space.

To simplify the analysis, it is assumed that $\epsilon = 1$ (corresponding closely to the experimental data) and that $\alpha = 1$ instead of the usual 0.93. Uncertainties of local albedo values and especially gross assumptions on the surface contour of the crater may introduce larger errors than the second assumption. In addition, reabsorption from the first and higher order reflections of the incident radiation may result in an effective α significantly higher than 0.93.

Analysis

In Fig. 1 incident heat flux at A_j from the sun and subsurface sources is

$$q_j = S_j + q_{sj} \tag{1}$$

and radiation leaving surface dA_i which is absorbed at surface dA_j is

$$dA_j q_{ij} = dA_i dF_{ij} J_i \tag{2}$$

The reciprocity relation states that

$$dA_i dF_{ij} = dA_j dF_{ji} \tag{3}$$

Combining Eqs. (2) and (3),

$$q_{ij} = J_i dF_{ji} \tag{4}$$

Furthermore, the diffuse form factor can be expressed as

$$dF_{ji} = K_{ji} dA_i \tag{5}$$

then

$$J_i dF_{ji} = K_{ji} dA_i J_i \tag{6}$$

where K_{ji} is the normalized form factor. The radiosity at A_j can be expressed as the sum of Eq. (1) and the contribution of radiation originated from all dA_i elements, which is the integral of Eq. (6) over the total crater surface:

$$J_j = q_j + \int_A K_{ji} J_i dA_i \tag{7}$$

This relation is Fredholm's integral equation of the second kind, which, in mathematical notation is

$$y(x) = f(x) + \lambda \int_a^b K(x, t) y(t) dt \tag{8}$$

where $y(x)$ is the unknown function (here, the radiosity of the

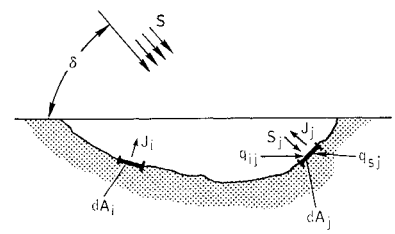

Fig. 1 Model of lunar crater for the heat balance equations.

Presented as Paper 69-595 at the AIAA Fourth Thermophysics Conference, San Francisco, Calif., June 16–18, 1969; submitted October 20, 1969; revision received December 22, 1969. The study was conducted for NASA by General Electric under Contract NASw-410.

* Consulting Engineer, Apollo Systems. Member AIAA

surface), $f(x)$ is a given function or the incident radiation and heat generation at the surface, $K(x, t)$ is the kernel of the integral equation or the normalized form factor, and λ is a given parameter. Solution methods[5,6] for these types of equations are quite complex, except for a few special cases.

The radiosities of the sunlit and shadowed regions, respectively, are (Fig. 2)

$$J_{1j} = q_{sj} + S_j + \xi \quad J_{2j} = q_{sj} + \xi \tag{9}$$

where

$$\xi = \lambda_1 \int_{A_1} K_{ji} J_{1j} dA_i + \lambda_2 \int_{A_2} K_{ji} J_{2i} dA_i \tag{10}$$

The foregoing equations are the governing relations for a black, partially shadowed cavity with arbitrary shape. In general, the four kernels are different, being functions of the geometry of the cavity and the relative size and location of the shadow. These kernels may cause difficulties in the solution of Eq. (8). Significant simplification can be obtained, however, by selecting a specific geometry, e.g., a spherical surface, for which the form factor between two surface elements, finite or infinitesimal, is constant, and the normalized form factor K_{ji} is

$$K_{ji} = dF_{ji}/dA_i = 1/(4\pi R^2) \equiv \lambda_0 \tag{11}$$

which is a constant quantity, depending only on the radius of the sphere.

Substituting Eq. (11) into Eq. (9), the governing euqations for radiosity and temperature of a shadowed spherical cavity can be obtained.

$$J_{1j} = S_j + q_{sj} + \lambda_0 \int_A J_i dA_i \tag{12}$$

and

$$J_{2j} = q_{sj} + \lambda_0 \int_A J_i dA_i \tag{13}$$

where J_i is not necessarily a continuous function.

Method of Solution

In order to solve Eqs. (12) and (13), the method of successive approximation will be applied by using the iterated kernels. It will be shown later that this method yields a closed form solution for the present problem. By the successive approximation method, the solution is given by an infinite series, known as Neumann's series,

$$J_j = q_i + (\lambda_0 + \lambda_0^2 A + \ldots + \lambda_0^n A^{n-1}) \int_A q_i dA_i \tag{14}$$

which can be written as

$$J_j = q_j + (\lambda_0 \int_A q_i dA_i)/(1 - A\lambda_0) \tag{15}$$

In general, the integral in the second term has to be performed in two parts, for the sunlit and the shadowed region.

$$\int_A q_i dA_i = \int_{A_1} (S_i + q_{si}) dA_i + \int_{A_2} q_{si} dA_i \tag{16}$$

which can be written as

$$\int_A q_i dA_i = \int_{A_1} S_i dA_i + \int_{A_2} q_{si} dA_i \tag{17}$$

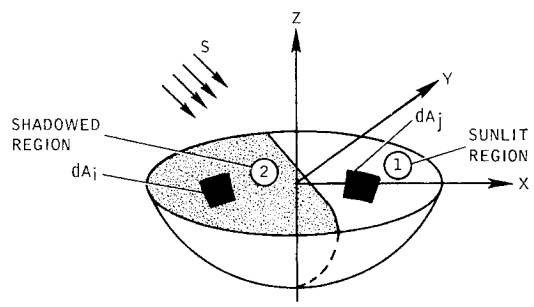

Fig. 2 Sunlit and shadowed regions of the lunar crater.

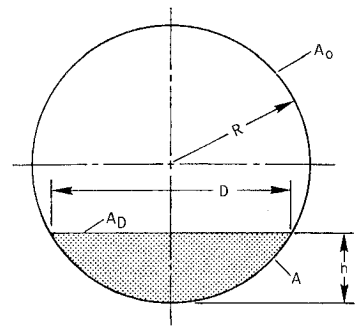

Fig. 3 Spherical geometry

The first term on the right-hand side represents the total incident solar energy on the cavity. Then

$$\int_A q_i dA_i = A_D S \sin\delta + A q_s \tag{18}$$

and the radiosity can be written by using $\lambda_0 = 1/4\pi R^2 = 1/A_0$, substituting this and Eq. (16) into Eq. (13),

$$J_j = q_j + [A_D/(A_0 - A)]S \sin\delta + [1/(A_0/A - 1)]q_s \tag{19}$$

By considering the spherical geometry of Fig. 3 and by introducing the aspect ratio of the crater as $a = D/h$, then

$$A_D/(A_0 - A) = (a^2/4 + 1)^{-1} \tag{20}$$

and

$$A_0/A = a^2/4 + 1 \tag{21}$$

which can be subscituted in Eq. (19).

Finally, the radiosities and surface temperatures of the sunlit and shadowed crater regions at arbitrary points are, respectively

$$J_1 = \sigma T_1^4 = S(\mathbf{s}\cdot\mathbf{n}) + \zeta \tag{22}$$
$$J_2 = \sigma T_2^4 = \zeta$$

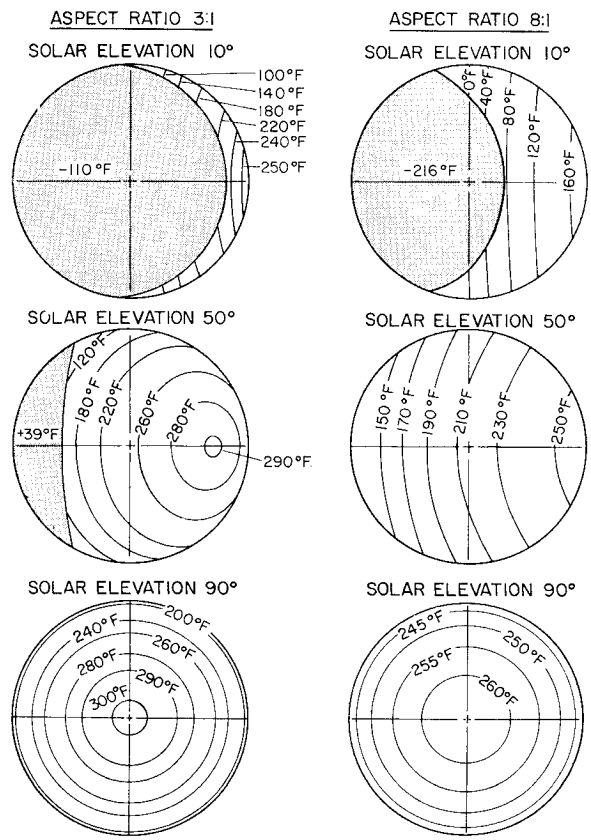

Fig. 4 Temperature distribution in spherical lunar craters.

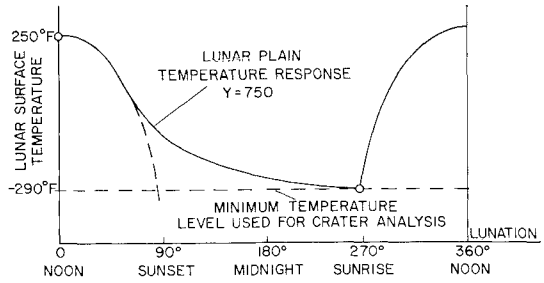

Fig. 5 Temperature response of the lunar surface.

where

$$\zeta \equiv (4/a^2 + 1)q_s + (S \sin\delta)/(a^2/4 + 1) \qquad (23)$$

and $\mathbf{s}\cdot\mathbf{n}$ is the scalar product of the solar ray unit vector $\mathbf{s}$ and crater surface unit normal vector $\mathbf{n}$.

Discussion of Results

The temperature relation for the shadowed region indicates that for the case of $q_s = 0$, the surface temperature of the crater approaches 0°R when $\delta = 0$, i.e., between sunset and sunrise points. This is not in agreement with lunar surface temperature data obtained by experimental methods. In effect, the minimum lunar surface temperature is not lower than ~170°R, because of the thermal inertia of the lunar soil. During the lunar day, the thermal energy penetrates into the soil and at night, it reverses the direction and flows toward the outside. As an approximation, the outward flowing heat can be considered as a surface source in the heat balance equation for lunar night and lunar shadow conditions. Taking T_s = 170°R as the minimum "level," the equivalent surface source is

$$q_s = \sigma T_s^4 = 1.4 \text{ Btu/hr-ft}^2$$

Figure 4 illustrates crater temperature distribution for 3:1 and 8:1 aspect ratio craters at various solar elevations. Shadow temperatures, which are constant, were computed based on the surface source approximation. It can be shown that by carrying on the source q_s in the computation of the crater temperatures in the sunlit region, the error introduced by the approximation is less than 1°R for $\delta = 90°$ and a 3:1 aspect ratio crater.

The black-body equilibrium temperature of the lunar plain at $\delta = 90°$ is approximately 250°F (710°R). In comparison, the maximum temperature in a 3:1 aspect ratio crater is 300°F, in an 8:1 crater, 260°F.

Figure 5 illustrates the surface source approximation to account for the thermal inertia of the lunar soil. The response curve was originally observed by Pettit and Nicholson[1] and later derived analytically by Jaeger.[2] Recent data obtained by Surveyor experiments are in good agreement with earlier findings,[3] with the exception of the numerical value of the thermal inertia. It was suggested to change this parameter from 750 cm²-sec$^{\frac{1}{2}}$-°C/cal to 500, although this change has only slight effect on the temperature response curve.

In addition to the more realistic prediction of lunar crater temperatures, the consideration of thermal inertia in the heat balance equations suggests a qualitative explanation of localized temperature variations on the lunar surface. Saari and Shorthill[7] observed that some craters cooled less rapidly than their surrounding regions. This anomaly was quite pronounced at some craters, especially at Tycho. Although Tycho is shallow, its surroundings are rough, covered with smaller craters and other topographical features with significantly lower aspect ratios. To clarify this question, however, the transient solution of the crater heat balance equation may be required.

References

[1] Pettit, E. and Nicholson, B., "Lunar Radiation and Temperatures," *Astrophysical Journal*, Vol. 71, 1930, pp. 102–135.

[2] Jaeger, J. C., "The Surface Temperature of the Moon," *Australian Journal of Physics*, Vol. 6, 1953, pp. 10–21.

[3] Lucas, J. W. et al., "Lunar Temperatures and Thermal Characteristics," *Surveyor III Mission Report, Part II*, TR 32-1177, June 1967, Jet Propulsion Lab., Pasadena, Calif., pp. 155–188.

[4] Lucas, J. W. et al., "Lunar Surface Temperatures and Thermal Characteristics," *Surveyor V Mission Report, Part II*, TR 32-1246, Nov. 1967, Jet Propulsion Lab., Pasadena, Calif., pp. 89–113.

[5] Volterra, V., *Leçons sur les Equations Intégrales et les Equations Intégrodifférentielles*, Gautier-Villars, Paris, 1913.

[6] Courant, R. and Hilbert, D., *Methods of Mathematical Physics*, Interscience, New York, 1966, Chap. 3, pp. 140–142.

[7] Saari, J. M. and Shorthill, R. W., "Isotherms of Crater Regions on the Illuminated and Eclipsed Moon," *Icarus*, Vol. 2, 1963, pp. 115–136.

Effects of Base Pressure on Conical Thrust Nozzle Optimization

C. Marshall Byington Jr.*
Naval Air Systems Command, Washington, D. C.
AND
Joe D. Hoffman†
Purdue University, Lafayette, Ind.

Nomenclature

A_p, A_s = nozzle plane and spherical exit area, respectively
A_t, A_b = nozzle throat area and missile base area, respectively
C_{F_M} = missile thrust coefficient = $F/P_c A_t$
D = missile diameter
F = thrust
L = nozzle length
$\dot{m}$ = mass flow rate
M_s, M_∞ = nozzle-exit and freestream Mach numbers
p_b, P_c = base pressure and nozzle stagnation pressure
p_o, p_s = ambient and nozzle exit pressure, respectively
r, r_o, r_b = p_s/P_c, p_o/P_c, and p_b/P_c, respectively
R = spherical exit area radius of curvature
T_o, T_c = stagnation temperatures, freestream and nozzle
y_e, y_t = nozzle-exit and throat radii
α = nozzle cone half-angle
γ = specific heat ratio
Γ $\equiv \gamma^{1/2}[2/(\gamma + 1)]^{(\gamma+1)/2(\gamma-1)}$
λ = divergence loss factor $\equiv (1 + \cos\alpha)/2$
ξ $\equiv [2\gamma/(\gamma - 1)]^{1/2}$
ρ_t = throat radius of curvature
ϵ = nozzle area ratio = A_p/A_t
ϵ_g = geometrical area ratio = A_s/A_t
ϵ_r = gasdynamic expansion ratio based on pressure ratio r
η = base pressure correlation function

Superscript

$*$ = variable nondimensionalized by throat radius

Introduction

It was shown by Scofield and Hoffman[1] that the adapted or fully expanded conical nozzle does not yield maximum thrust, and the condition for maximum thrust was derived. However, in Ref. 1 and other studies which consider the design of a thrust nozzle alone, ambient pressure is generally assumed to surround the nozzle, and the effects that a flight ve-

Received December 22, 1969.
* Project Engineer. Student Member AIAA.
† Associate Professor of Mechanical Engineering. Member AIAA.